Microhydration of NO_3^-: A Theoretical Study on Structure, Stability and IR Spectra

A. K. Pathak,† T. Mukherjee,† and D. K. Maity*,‡

Radiation and Photochemistry Division, and Theoretical Chemistry Section, Chemistry Group, Bhabha Atomic Research Centre, Mumbai 400085, India

Received: November 22, 2007; In Final Form: January 17, 2008

A systematic study on the structure and stability of nitrate anion hydrated clusters, $NO_3^-{\cdot}nH_2O$ ($n = 1-8$) are carried out by applying first principle electronic structure methods. Several possible initial structures are considered for each size cluster to locate equilibrium geometry by applying a correlated hybrid density functional with 6-311++G(d,p) basis function. Three different types of arrangements, namely, symmetrical double hydrogen bonding, single hydrogen bonding and inter-water hydrogen bonding are obtained in these hydrated clusters. A structure having inter-water hydrogen bonding is more stable compared to other arrangements. Surface structures are predicted to be more stable over interior structures. Up to five solvent H_2O molecules can stay around solute NO_3^- anion in structures having an inter-water hydrogen-bonded cyclic network. A linear correlation is obtained for weighted average solvent stabilization energy with the size (n) of the hydrated cluster. Distinctly different shifts of IR bands are observed in these hydrated clusters for different kinds of bonding environments of O−H and N═O stretching modes compared to isolated H_2O and NO_3^- anion. Weighted average IR spectra are calculated on the basis of statistical population of individual configurations of each size cluster at 150 K.

1. Introduction

Size selected gas-phase cluster spectroscopy combined with first principles based theoretical calculations has become a powerful tool to obtain molecular level information on the interaction between solute and solvent molecules. Positively charged ions have simple hydrated structures compared to a negatively charged system as cation binds strongly with solvent water molecules.[1] In recent years, the study on microhydration of small anionic chemical species has been a subject of intense research from both experimental and theoretical points of view, mainly because of the strong dependency of their properties on their size and geometry. When an anionic solute is immersed into a solvent pool, the hydrogen-bonded water network gets modified to accommodate the solute species in the process of hydration. The distribution pattern of the excess electron in the negatively charged solute plays the key role to shape up the structure of the water network around the solute. Thus, a delicate balance between anion−water and water−water interactions determines the structure of hydrated clusters of the anion. Among the simplest of the systems studied by experimental and theoretical tools is the hydrated halide series, $X^-{\cdot}nH_2O$, (X = Cl, Br, I). Several experiment, theory and simulation studies have been carried out to understand the structure and dynamic aspects of hydration at molecular level on small negatively charged ions.[1−21] Beyond these simple halide anions, the next complex hydrated clusters investigated involve diatomic singly charged anions of the type $Y^-{\cdot}nH_2O$, where Y refers to OH,[21,22] O_2,[23,24] NO,[25] Cl_2,[26,27] Br_2[28,29] and I_2[30] species. Microhydration of a dianionic system, SO_4^{2-} has also been studied to demonstrate the stepwise hydration pattern of these complex anion systems.[31−33] At present, microhydration of another complex but the most common inorganic anion, namely, nitrate anion (NO_3^-) is studied by theoretical means. This anion is one of the most abundant species in acidic wastes as well as in the atmosphere.[34−37] It is known as the so-called terminal anion in the series of atmospheric reactions involving nitrogen and thus its study is of particular importance. The process of hydration involving nitrate anion in the atmosphere is very important, as water is present in the atmosphere in relatively large concentrations. Such a study will help to enhance our understanding of molecular level interactions between solvent water molecules and negatively charged ions in aqueous solution. These studies on size selected hydrated anion clusters also play a critical role to follow the evolution of molecular properties with the number of solvent water molecules present in the cluster and to bridge the gap between monohydrated cluster ($NO_3^-{\cdot}H_2O$) to the hydrated ion in bulk aqueous solution, NO_3^-(aq).

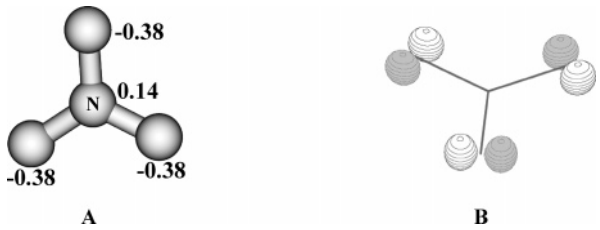

Figure 1. (A) Fully optimized structures of NO_3^- calculated at the B3LYP/6-311++G(d,p) level of theory showing distribution of charge over all the atoms. (B) Contour plot of the highest occupied molecular orbital (HOMO) of NO_3^- to show that all the three O atoms participate in the orbital. The cutoff used for the contour plot is 0.25 au.

Theoretical studies on structural aspects of small size $NO_3^-{\cdot}nH_2O$ clusters are reported.[38−44] However, no report on IR spectra of these clusters is available in the literature. The objective of this article is to report microscopic structure, energy parameters and IR spectra of $NO_3^-{\cdot}nH_2O$ clusters ($n = 1-8$) based on a rigorous and systematic study. With the increase in

* Corresponding author. E-mail for correspondence: dkmaity@barc.gov.in.
† Radiation and Photochemistry Division.
‡ Theoretical Chemistry Section.

10.1021/jp711108q CCC: $40.75
Published on Web 03/08/2008

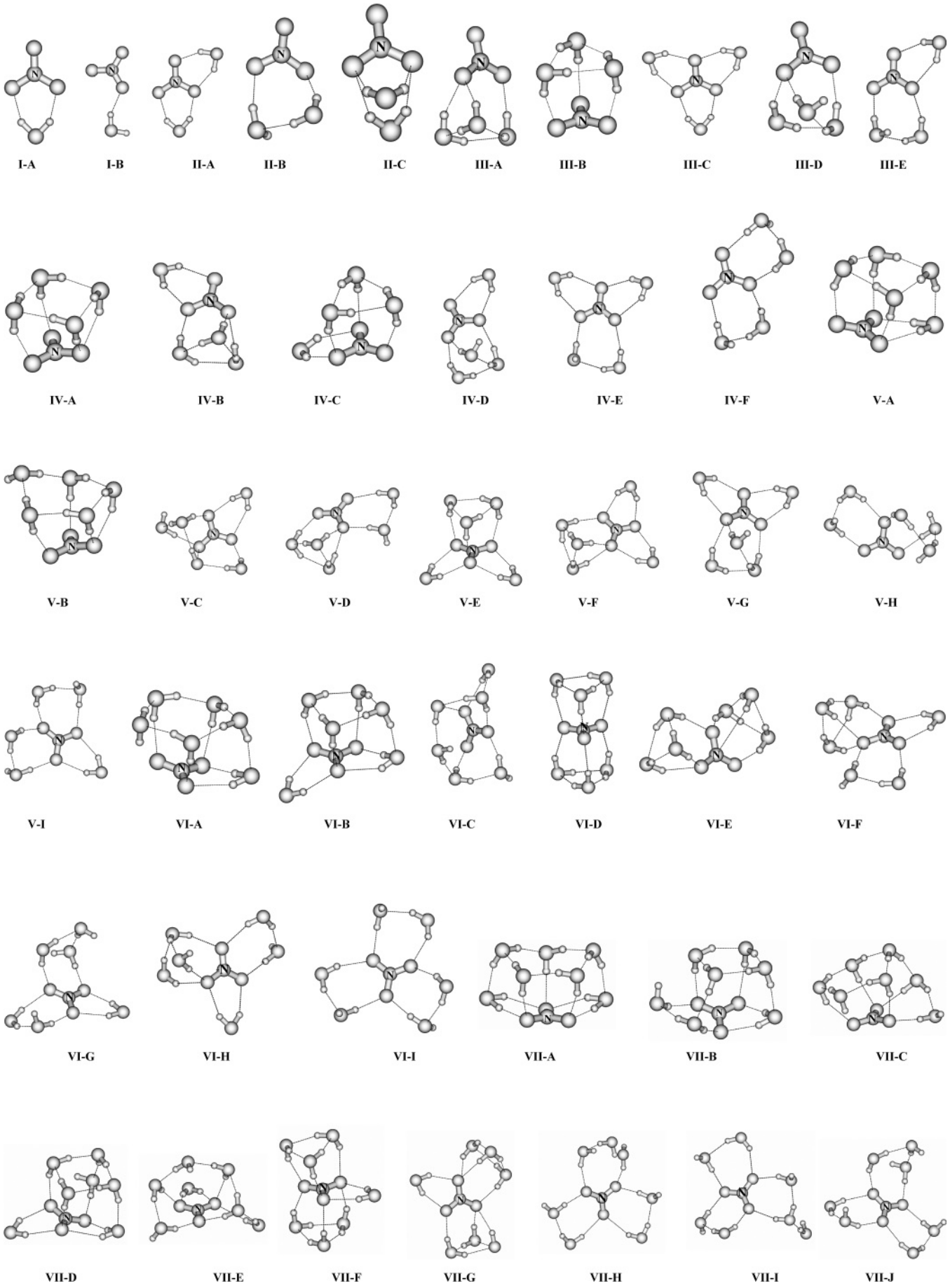

Figure 2. Part 1 of 2.

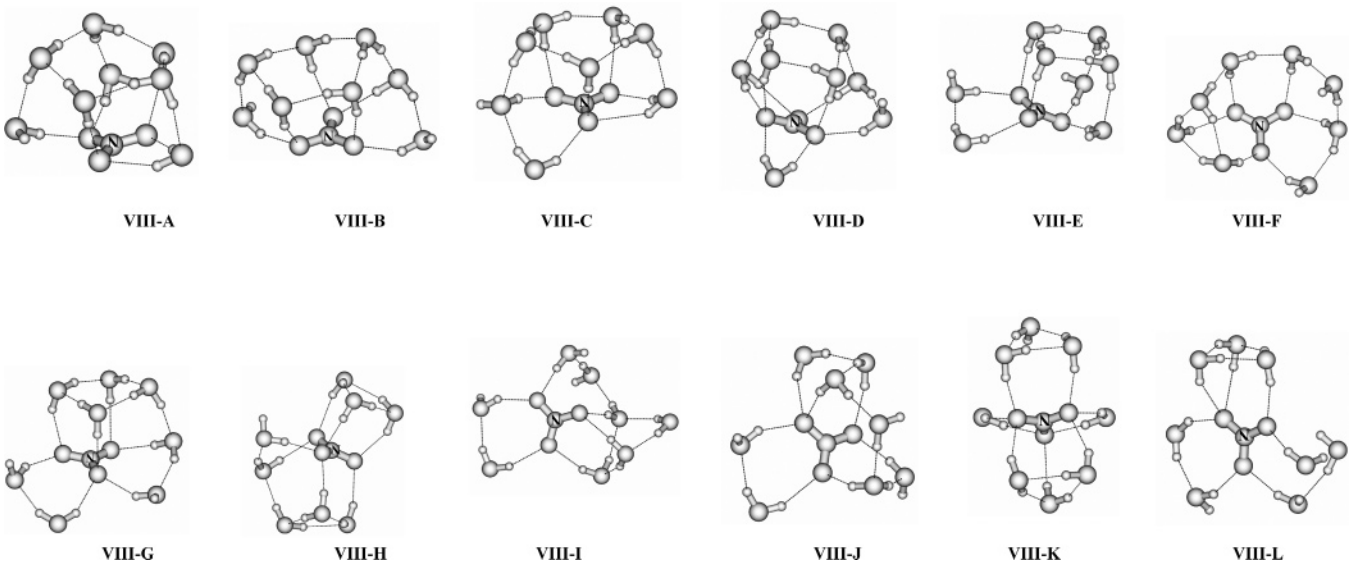

Figure 2. Part 2 of 2. Fully optimized structures calculated at B3LYP/6-311++G(d,p) level of theory for (I) $NO_3^-\cdot H_2O$, (II) $NO_3^-\cdot 2H_2O$, (III) $NO_3^-\cdot 3H_2O$, (IV) $NO_3^-\cdot 4H_2O$, (V) $NO_3^-\cdot 5H_2O$, (VI) $NO_3^-\cdot 6H_2O$, (VII) $NO_3^-\cdot 7H_2O$, and (VIII) $NO_3^-\cdot 8H_2O$ clusters. Uppercase letters are used to refer different minimum energy conformers for each hydrated cluster size arranged in order of stability showing "A" as the most stable one. N atoms are shown by marking "N" on the spheres; the smallest spheres refer to H atoms, and the rest correspond to O atoms in each structure. In each case, the distance between the N and O atoms is ~1.25 Å, the distance between O of NO_3^- and H-bonded H atoms is 1.8−2.3 Å, and the distance between O and H atoms in inter-water hydrogen-bonded network is 1.8−2.0 Å.

number of solvent water molecules in hydrated clusters, the number of minimum energy configurations that are close in energy for each size hydrated clusters is expected to increase. Thus, weighted average properties of clusters become more meaningful. Weighted average molecular properties are also calculated at present on the basis of the statistical population of different minimum energy configurations of a particular size of hydrated cluster at 150 K.

2. Theoretical Methods

Geometry optimizations are carried out following a popular hybrid density functional, namely, Becke's three-parameter nonlocal exchange (B3) and Lee−Yang−Parr (LYP) nonlocal correlation functionals (B3LYP) with the Gaussian triple split valence, 6-311++G(d,p) basis function.[45] Single-point energy calculations of each optimized structure are carried out by applying second-order Møller−Plesset perturbation theory (MP2) adopting the same set of basis function. A search for minimum energy structures is performed by applying an algorithm based on the Newton−Raphson procedure for each of these molecular clusters with several initial structures designed on the basis of chemical intuition. The most important concern in this search procedure is to guess a good initial geometry of the cluster based on chemical intuition, which might converge during the optimization to a structure having a local or the global energy minima. At present, several possible starting geometries are designed systematically on the basis of different possible three-dimensional structures. In the *first* case, initial structures are considered where each solvent water molecule was kept at a distance of ionic hydrogen bonding with one of the three oxygen atoms of NO_3^- anion and far from another solvent water molecule to have any inter-water hydrogen bonding. In the *second* case, guess structures were considered where each water molecule was kept at a distance of ionic hydrogen bonding with one of the three oxygen atoms of NO_3^- anion and also at a distance to have an inter-water hydrogen bonding with another solvent H_2O molecule. In the *third* case, a few solvent water molecules were initially kept at a distance of ionic hydrogen bonding with one of the three oxygen atoms of NO_3^- anion and far from another solvent water molecule to have any inter-water hydrogen bonding. Remaining solvent water molecules were kept at a distance of ionic hydrogen bonding with one of the three oxygen atoms of NO_3^- and also at a distance where inter-water hydrogen-bonding interaction can exists. These structures were then allowed to relax, producing equilibrium minimum energy structures. It is to be noted that the adopted optimization procedure does not guarantee locating the global minimum energy structure. However, rigorous searches have been undertaken to find all possible equilibrium structures that may exist for $NO_3^-\cdot nH_2O$ systems. Hessian calculations are carried out for all the optimized minimum energy structures to check the nature of the equilibrium geometry as well as to generate IR spectra. The population of the minimum energy configurations of each size clusters has been calculated on the basis of free energy change (ΔG) at 150 K following Boltzmann distribution. The statistical population of different equilibrium structures is calculated at various temperatures ranging from 75 to 298 K. The weighted average properties are reported only at 150 K as the size selected clusters spectroscopy experiments on such systems are mostly carried out at around this temperature. All electronic structure calculations have been carried out applying GAMESS program system on a LINUX cluster platform.[46] The MOLDEN program system has been adopted for visualization of molecular geometry, molecular orbital, and normal modes and to generate IR spectra.[47]

3. Results and Discussion

Geometry optimization of isolated nitrate anion in the gas phase, NO_3^- produces a structure of D_{3h} symmetry as the most stable structure by applying the B3LYP density functional with a Gaussian split valence 6-311++G(d,p) basis set. The calculated N−O bond distance is 1.261 Å and the optimized structure with atomic charges (in au) over the atoms is displayed in Figure 1A to illustrate that all the three oxygen atoms are equally negative. The highest occupied molecular orbital (HOMO) of

NO_3^- system is displayed in Figure 1B, again to demonstrate that all the three O atoms participate equally in this molecular orbital. The effect of hydration is introduced by successive addition of discrete solvent H_2O molecules surrounding NO_3^- species. When a solvent H_2O molecule approaches the solute NO_3^- moiety, an ionic interaction between the negatively charged oxygen atom of NO_3^- and the H atom of solvent H_2O takes place. Discrete water molecules are added successively to the solute by various possible ways based on chemical intuition as discussed in the previous section, and full geometry optimization is carried out to locate equilibrium structures at the B3LYP/6-311++G(d,p) level of theory. This leads to several minimum energy structures for each of the discrete hydrated clusters. The calculated energy parameters are improved by single-point energy calculations at MP2 level of theory. Minimum energy configurations, various energy parameters and IR spectra of each size hydrated cluster, $NO_3^-\cdot nH_2O$ ($n = 1-8$) are discussed in the following subsections.

3.1. Structure. Different minimum energy structures obtained on full geometry optimization of each size hydrated cluster of nitrate anion, $NO_3^-\cdot nH_2O$ ($n = 1-8$) are displayed in Figure 2. The calculated energy parameters are listed in Table 1 for each minimum energy structure of the hydrated clusters. Two stable minimum energy structures are obtained on full geometry optimization of the monohydrate cluster, $NO_3^-\cdot H_2O$ as shown in Figure 2-I(A,B). In contrast to the earlier reported structure,[39] the most stable structure has a symmetric double-hydrogen-bonding (DHB) arrangement where two O atoms from NO_3^- group and two H-atoms of the solvent H_2O molecule are connected by H-bonding of 2.06 Å. Calculated NO bond distances are 1.25 and 1.27 Å, respectively, for the spectator and H-bonded bonds. Structure I-B having one single hydrogen bond (SHB) between one oxygen atom of the nitrate anion and the H atom of the solvent H_2O molecule is less stable than structure I-A by 2.78 kcal/mol. The calculated H-bond distance is 1.83 Å, and so this SHB should be stronger than each DHB of structure I-A. Again, NO bond distances are 1.25 and 1.27 Å, respectively, for the spectator and H-bonded bonds. Hessian calculations have predicted all the normal-mode frequencies to be real. The calculated binding enthalpy (ΔH) of the more stable structure I-A is 14.68 kcal/mol at 298.15 K. The reported experimental ΔH for the monohydrated cluster is 14.60 kcal/mol measured by gas-phase clustering equilibrium experiment at room temperature.[48] Binding enthalpies of the monohydrated cluster calculated by applying BHHLYP hybrid density functional and MP2 methods are 14.49 and 14.76 kcal/mol, respectively. The calculated values suggest that the present adopted hybrid density functional, namely, B3LYP, should be adequate for the present systems. To further validate the suitability of this particular functional, vertical detachment energy (VDE) of the monohydrate cluster, $NO_3^-\cdot H_2O$ is also calculated following these two popular hybrid density functionals as well as MP2 methods with 6-311++G(d,p) basis functions. The calculated VDE values are 4.93, 5.33 and 4.08 eV, respectively at B3LYP, BHHLYP and MP2 levels compared to the measured value of 4.6 eV following photodetachment photoelectron spectroscopy.[38] Again, it is observed that B3LYP functional performs well on these hydrated clusters. Thus geometry optimizations and Hessian calculations of all these hydrated clusters have been carried out by applying the cost-effective correlated B3LYP hybrid density functional.

Three minimum energy structures are predicted for the dihydrate cluster, $NO_3^-\cdot 2H_2O$ and displayed in Figure 2-II(A–C). The structures are very close in energy with a difference in

TABLE 1: Calculated Energy Parameters and Molecular Properties of $NO_3^-\cdot nH_2O$ Clusters ($n = 1-8$)[a]

		energy (kcal/mol)		
system	population at 150 K	relative energy,[b] ΔE	solvent stabilization[c] energy, E^{solv}	interaction energy,[c,d] E^{int}
		$NO_3^-\cdot H_2O$		
I-A	0.59	0	16.31, *16.44*	17.05, *17.18* (15.40)
I-B	0.41	2.78	13.53, *13.60*	14.07, *14.11* (12.70)
		$NO_3^-\cdot 2H_2O$		
II-A	0.50	0	30.82, *31.10*	32.47, *32.71* (30.67)
II-B	0.23	1.31	29.51, *29.71*	27.77, *27.84* (26.29)
II-C	0.27	1.95	28.87, *29.20*	31.12, *31.32* (29.00)
		$NO_3^-\cdot 3H_2O$		
III-A	0.41	0	44.02	37.50 (35.52)
III-B	0.29	0.26	43.76	33.00 (30.76)
III-C	0.11	0.39	43.63	46.67 (44.09)
III-D	0.14	0.66	43.36	39.62 (37.19)
III-E	0.05	1.04	42.98	42.57 (40.05)
		$NO_3^-\cdot 4H_2O$		
IV-A	0.68	0	59.90	42.44 (39.66)
IV-B	0.10	3.35	56.55	50.71 (47.91)
IV-C	0.11	3.58	56.32	47.30 (44.09)
IV-D	0.04	3.98	55.92	53.43 (50.06)
IV-E	0	4.86	55.04	55.23 (52.16)
IV-F	0.07	5.16	54.74	50.90 (47.90)
		$NO_3^-\cdot 5H_2O$		
V-As	0.51	0	74.29	51.30 (48.09)
V-B	0.30	2.29	72.00	45.81 (42.90)
V-C	0.03	5.88	68.41	59.98 (56.15)
V-D	0.07	6.53	67.76	59.71 (56.54)
V-E	0.02	6.77	67.52	60.37 (56.24)
V-F	0.05	6.82	67.47	62.91 (59.36)
V-G	0	7.67	66.62	64.83 (60.93)
V-H	0.01	7.69	66.60	58.38 (54.84)
V-I	0.01	8.30	65.99	63.78 (60.08)
		$NO_3^-\cdot 6H_2O$		
VI-A	0.73	0	87.09	59.11 (55.49)
VI-B	0.05	1.90	85.19	63.51 (59.41)
VI-C	0.07	5.61	81.48	59.87 (56.79)
VI-D	0.10	5.94	81.15	60.17 (55.85)
VI-E	0.03	7.53	79.56	65.88 (65.28)
VI-F	0.01	8.93	78.16	70.95 (67.00)
VI-G	0	9.80	77.28	68.48 (64.33)
VI-H	0.01	9.89	77.20	71.59 (67.26)
VI-I	0	11.03	76.06	70.90 (67.01)
		$NO_3^-\cdot 7H_2O$		
VII-A	0.25	0	100.69	67.32 (63.24)
VII-B	0.31	1.01	99.68	66.91 (62.95)
VII-C	0.20	2.31	98.38	65.80 (61.86)
VII-D	0.08	3.38	97.31	70.60 (66.09)
VII-E	0	8.78	91.91	71.02 (66.44)
VII-F	0.05	10.43	90.26	72.26 (67.08)
VII-G	0.11	11.36	89.33	76.43 (72.07)
VII-H	0	13.31	87.38	76.95 (72.84)
VII-I	0	14.00	86.69	75.15 (71.26)
VII-J	0	14.20	86.49	74.70 (70.45)
		$NO_3^-\cdot 8H_2O$		
VIII-A	0.11	0	112.10	73.50 (69.15)
VIII-B	0.34	1.22	110.88	72.53 (68.30)
VIII-C	0.09	1.68	110.42	73.91 (69.44)
VIII-D	0.07	3.13	108.97	77.39 (72.68)
VIII-E	0.07	4.11	107.99	77.08 (72.20)
VIII-F	0.13	5.04	107.06	72.36 (68.29)
VIII-G	0.08	5.44	106.66	76.80 (72.11)
VIII-H	0.04	7.33	104.77	76.12 (71.00)
VIII-I	0.02	9.67	102.43	77.43 (73.19)
VIII-J	0.01	10.07	102.03	77.27 (72.43)
VIII-K	0	13.16	98.94	81.03 (75.42)
VIII-L	0.04	13.58	98.52	81.57 (77.09)

[a] Energy values are calculated at the MP2/6-311++G(d,p) level of theory. [b] ΔE = relative energy (energy of any structure − energy of structure A in $NO_3^-\cdot nH_2O$ system). [c] Data in italics refer to values calculated at CCSD(T)/6-311++G(d,p) level. [d] Values in parentheses refer to basis set superposition error (BSSE)-corrected data.

relative stability of <2 kcal/mol. Structures II-A and II-C have two double-hydrogen-bonding (DHB) arrangements and both solvent H_2O units are attached to the same two O atoms of NO_3^- in case of the less stable structure II-C. In case of II-C, none of the solvent H_2O units is in NO_3^- plane, structure II-A is planar though. Structure II-B has two single hydrogen-bonding (SHB) and one inter-water hydrogen-bonding (WHB) arrangements.

Five minimum energy structures displayed in Figure 2-III-(A-E) are predicted for trihydrate cluster, $NO_3^-\cdot 3H_2O$ and have a very small difference in stability as listed in Table 1. Structure III-A is the most stable one having a cyclic three-member water network attached to two oxygen atoms of NO_3^- moiety. This particular structure consisting three SHB and three WHB arrangements is more stable than the least stable structure III-E having two SHB, one DHB and one WHB arrangements by only ~1 kcal/mol. Structure III-B consisting of a cyclic three-member water network attached to all the three oxygen atoms is less stable than structure III-A by 0.26 kcal/mol. Symmetric structure III-C having three DHB arrangements is 0.39 kcal/mol less stable compared to the most stable one. Structure III-D consisting of three SHB and two WHB arrangements is less stable by 0.66 kcal/mol compared to structure III-A. On the basis of the optimized structures up to $NO_3^-\cdot nH_2O$ ($n = 1-3$), it is observed that the average energies of a single SHB and WHB arrangements are 7−11 and 5−8 kcal/mol, respectively. So a balance between water−NO_3^- and water−water interactions decides the structure of hydrated anion clusters, $NO_3^-\cdot nH_2O$.

As the number of solvent water molecules increases, a large number of minimum energy configurations is expected for a particular size of hydrated cluster. The initial structures for larger hydrated clusters are considered with a bottom-up approach based on the predicted stable structures from the smaller size hydrated clusters. Thus the initial guess structures for $NO_3^-\cdot 4H_2O$ cluster are considered on the basis of the predicted minimum energy structures of $NO_3^-\cdot nH_2O$ clusters ($n = 1-3$), keeping a different number of symmetrical DHB, SHB and WHB arrangements. Six stable minimum energy structures are obtained for $NO_3^-\cdot 4H_2O$ cluster. The calculated relative stability of the predicted conformers are listed in Table 1 and the optimized structures are displayed in Figure 1-IV(A-F). Structure IV-A is more stable over the least stable conformer, IV-F, by 5.16 kcal/mol. Structure IV-A consists of a four-member cyclic water network with four SHB and four WHB arrangements. But the structure IV-F consists of four SHB and two WHB arrangements. Structures IV-B and IV-C consist of one cyclic three-member water network and one DHB water arrangements. Structure IV-D has one DHB, three SHB and two WHB arrangements. As one can see from the figure, structure IV-E has two DHB, two SHB and one WHB arrangements. At present no structure for the $NO_3^-\cdot 4H_2O$ cluster is obtained where all four solvent water units are in DHB arrangements.

Geometry optimization followed by Hessian calculations with various initial guess structures for the pentahydrate cluster, $NO_3^-\cdot 5H_2O$ yields nine minimum energy structures having no imaginary frequency and the structures are displayed in Figure 2-V(A−I). The most stable structure, V-A, consists of one DHB arrangement and one cyclic four-member water network. Overall, four SHB, four WHB and one DHB arrangements are present in structure V-A. Structure V-B consisting of one five-member water network is less stable than the most stable conformer by 2.29 kcal/mol. Structure V-I is the least stable conformer, which is less stable than the most stable conformer, V-A, by 8.30 kcal/mol. Structure V-I consists of one DHB, five SHB and two WHB arrangements. Structures V-D, V-E and V-F have one cyclic three-member water network. Remaining conformers have different numbers of DHB, SHB and WHB arrangements. As can be seen from Table 1, structures V-(C−I) are very close in energy (<2.42 kcal/mol).

Nine different minimum energy structures displayed in Figure 1-VI(A−I) having all real frequency are obtained for $NO_3^-\cdot 6H_2O$ cluster. The most stable structure of $NO_3^-\cdot 6H_2O$ cluster (VI-A) has one DHB and one cyclic five-member water network arrangements. In total, it has one DHB, four SHB and five WHB arrangements. This structure is more stable than the least stable structure VI-I by 11.03 kcal/mol. Structure VI-I has six SHB and three WHB arrangements. Structure VI-B having two DHB and one cyclic four-member water network arrangements is less stable than structure VI-A by 1.90 kcal/mol. Structures VI-D and VI-E both have two cyclic three-member water networks, and structure VI-F has one cyclic three-member water network arrangement. These are two interior 3D structures in which the solute is surrounded by two H-bonded solvent water networks. In the case of the minimum energy structure VI-G, a solvent water molecule is not directly connected to the NO_3^- moiety, though all six water molecules were kept directly connected to the NO_3^- moiety in the initial guess structure. Structure VI-G has one DHB, four SHB and two WHB arrangements.

Ten minimum energy configurations are predicted for the $NO_3^-\cdot 7H_2O$ cluster and finally the optimized structures are displayed in Figure 1-VII(A−J). Hessian calculations do not produce any normal mode having imaginary frequency for these structures. This confirms that the predicted minimum energy configurations correspond to true equilibrium structures of $NO_3^-\cdot 7H_2O$ cluster. The most stable structure, VII-A, has a cyclic five-member water network arrangement and the solute anion, NO_3^-, resides at the surface. Similar geometrical arrangements keeping the solute at the surface are also observed in case of structures VII(B−E) and VII(H−J). Interior structures in which the solute is surrounded by solvent water units are predicted for two minimum energy configurations, VII(F,G).

On full geometry optimization of $NO_3^-\cdot 8H_2O$ cluster, twelve minimum energy structures are predicted and the final optimized structures are displayed in Figure 1-VIII(A−L). None of these structures yields an imaginary frequency on Hessian calculations, suggesting these minimum energy configurations as true equilibrium structures. As in case of the heptahydrated cluster, the most stable structure has a cyclic five-member water network arrangement keeping the solute anion at the surface. Similar geometrical arrangements keeping the solute at the surface are also observed in the remaining of structures except for the structures VIII-H and VIII-K. In these two cases, NO_3^- trapped inside H-bonded solvent water networks.

In all the minimum energy configurations of $NO_3^-\cdot nH_2O$ cluster, the NO bond distance is calculated in the range 1.25−1.27 Å. The calculated distance between O of NO_3^- and H-bonded H atoms is 1.8−2.3 Å, and the distance between O and H atoms in the inter-water network (WHB) is 1.8−2.0 Å. In all the structures, the calculated SHB distance is shorter than that of DHB distance. Structure having cyclic inter-water H-bonding network is more stable over other structures in a particular size of hydrated cluster. It is observed that more than three solvent water molecules cannot reside in a DHB arrangement in these hydrated clusters. It is also observed that more than five water molecules cannot stay in the cyclic water network. Most of the minimum energy configurations in $NO_3^-\cdot nH_2O$ cluster show surface structure in which the solute resides at the surface of the solvent water network. In the case of large size hydrated clusters, $NO_3^-\cdot nH_2O$ ($n \geq 6$), a few

TABLE 2: Calculated Weighted Average Molecular Properties of $NO_3^-{\cdot}nH_2O$ ($n = 1-8$) Clusters at the MP2/6-311++G(d,p) Level of Theory

	weighted average property energy (kcal/mol)	
hydrated cluster	solvent stabilization energy, E_w^{solv}	interaction energy,[b] E_w^{int}
$NO_3^-{\cdot}H_2O$	15.17	15.83 (14.29)
$NO_3^-{\cdot}2H_2O$	29.99	31.02 (29.21)
$NO_3^-{\cdot}3H_2O$	42.46	37.75 (35.54)
$NO_3^-{\cdot}4H_2O$	58.65	44.83 (41.97)
$NO_3^-{\cdot}5H_2O$	72.33	51.46 (48.28)
$NO_3^-{\cdot}6H_2O$	85.59	59.94 (56.25)
$NO_3^-{\cdot}7H_2O$	97.87	68.40 (64.27)
$NO_3^-{\cdot}8H_2O$	108.81	74.39 (69.98)

[b] Values in parentheses are basis set superposition error (BSSE) corrected.

equilibrium geometries are predicted showing interior structure in which the solute resides inside the solvent water network. However, surface structures are observed to be more stable than corresponding interior structures.

3.2. Solvent Stabilization and Interaction Energy. The solvation stabilization energy (E^{solv}), i.e., the stabilization induced by solvent water molecules of $NO_3^-{\cdot}nH_2O$ clusters can be expressed by the relation given in

$$E^{solv} = E_{NO_3^-.nH_2O} - (nE_{H_2O} + E_{NO_3^-}) \quad (1)$$

The energy parameters $E_{NO_3^-{\cdot}nH_2O}$, E_{H_2O}, and $E_{NO_3^-}$ refer to the total energy of the cluster $NO_3^-{\cdot}nH_2O$, the energy of a single H_2O molecule and the energy of the bare NO_3^- system, respectively. Thus, E^{solv} essentially measures the total interaction energy of the solute with n solvent H_2O units in the hydrated cluster of size n. The calculated solvation energy of the $NO_3^-{\cdot}nH_2O$ clusters ($n = 1-8$) at the MP2/6−3111++G(d,p) level of theory is given in Table 1. As a number of minimum energy configurations are obtained in these hydrated clusters, weighted average solvation energy (E_w^{solv}) values are calculated and provided in Table 2. The weight factor of a minimum energy structure for a particular size (n) of cluster is calculated on the basis of the statistical population of the conformer at 150 K. The plot for the variation of E_w^{solv} vs n (cluster size) is depicted in Figure 3a. It is observed that E_w^{solv} varies linearly with the number of solvent water molecules in the hydrated clusters and the variation of E_w^{solv} is best fitted as $E_w^{solv} = 2.89 + 13.55n$, when E_w^{solv} is expressed in kcal/mol and n is the number of water molecules. This linear fitted plot has a correlation coefficient greater than 0.999, promising the power of prediction of solvent stabilization energy for larger hydrated clusters. The slope of the best fitted equation suggests that solvent stabilization energy per solvent water unit is 13.55 kcal/mol. In other words, on an average each additional H-bond provides a stabilization of 6.77 kcal/mol at a large n limit, assuming each additional solvent water molecule to increase the number of H-bonds by 2. However, this assumption is true for a very large size (n) of cluster. A small correction is expected in H-bond stabilization energy if one goes to very large size hydrated clusters. The solvent stabilization energy of $NO_3^-{\cdot}nH_2O$ clusters calculated by a discrete model corresponds to the internal energy of the molecular clusters. Thus, E_w^{solv} increases with the increase in the number of solvent molecules accounting for ion−solvent interaction as well as inter-water H-bonding interaction. In other words, solvent stabilization energy does not saturate because it remains favorable to attach additional water molecules to the existing water network.

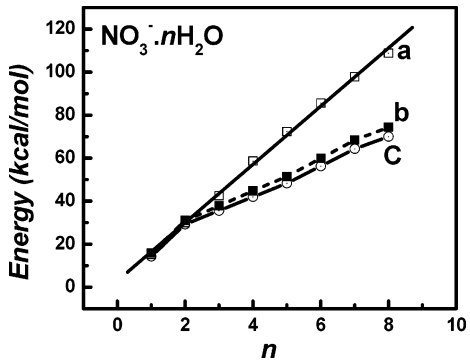

Figure 3. Variation of calculated weighted average (a) solvation energy (E_w^{solv}) and (b) interaction energy (E_w^{int}) in kcal/mol with the number of water molecules (n) in $NO_3^-{\cdot}nH_2O$ cluster at the MP2/6-311++G-(d,p) level of theory. In estimation of E_w^{solv} and E_w^{int}, the weight factor is calculated on the basis of the statistical population of all the conformers for each size of hydrated cluster at 150 K. Variation of (c) BSSE-corrected E_w^{int} (kcal/mol) vs the number of solvent water molecules (n) in the $NO_3^-{\cdot}nH_2O$ cluster at the same level of theory. The calculated correction due basis set superposition error following counterpoise method is ≤5%.

The interaction between the solute nitrate ion, NO_3^-, and the water cluster, $(H_2O)_n$, known as interaction energy (E^{int}) may be calculated by the following relation.

$$E^{int} = E_{NO_3^-{\cdot}nH_2O} - (E_{(H_2O)_n} + E_{NO_3^-}) \quad (2)$$

The energy parameters $E_{NO_3^-{\cdot}nH_2O}$, $E_{(H_2O)_n}$ and $E_{NO_3^-}$ refer to the energy of the cluster $NO_3^-{\cdot}nH_2O$, the energy of the $(H_2O)_n$ system and the energy of the NO_3^- system, respectively. The energy of the $(H_2O)_n$ system is calculated by removing the nitrate part from the optimized geometry of the hydrated cluster followed by single-point energy calculation at the same level of theory. $E_{NO_3^-}$ is also evaluated by the same way, i.e., by removing the water part of the optimized structure of the hydrated cluster followed by single-point energy calculation. The definition suggests that the interaction energy refers to the net interaction of solute NO_3^- anion and the solvent water molecules eliminating inter-water interactions. The calculated interaction energy for the $NO_3^-{\cdot}nH_2O$ cluster ($n = 1-8$) is tabulated in Table 1. The weighted average interaction energy, E_w^{int}, is also calculated for all sizes of the hydrated clusters on the basis of the statistical population at 150 K, and the results are supplied in Table 2. The plot showing the variation of E_w^{int} vs n is displayed in Figure 3b. It is clearly seen from the plots in Figure 3 that the interaction energy is very close to the solvation energy for $n = 1-2$. This is due to absence of inter-water hydrogen bonding (DHB) in the most stable structures of $NO_3^-{\cdot}nH_2O$ clusters ($n = 1-2$). However, for large size clusters, a calculated interaction energy is much lower than the solvation energy because, in the higher clusters, additional solvent water molecules mostly interact with the water network of the cluster. The calculated profile does not reach a saturation showing that the solute nitrate anion has significant interaction even with the eighth solvent water unit suggesting incomplete first solvation shell. It is evident that the coordination number of NO_3^- hydration is more than 8. Once the number of solvent water units is more than the first shell hydration number of NO_3^-, the cluster will grow by inter-water H-bond only showing saturation in interaction energy profile. It is to be noted that both energy parameters (E^{sol} and E^{int}) are also calculated by the CCSD(T) method with the same set of basis function for mono- and dihydrated clusters and the values are displayed in

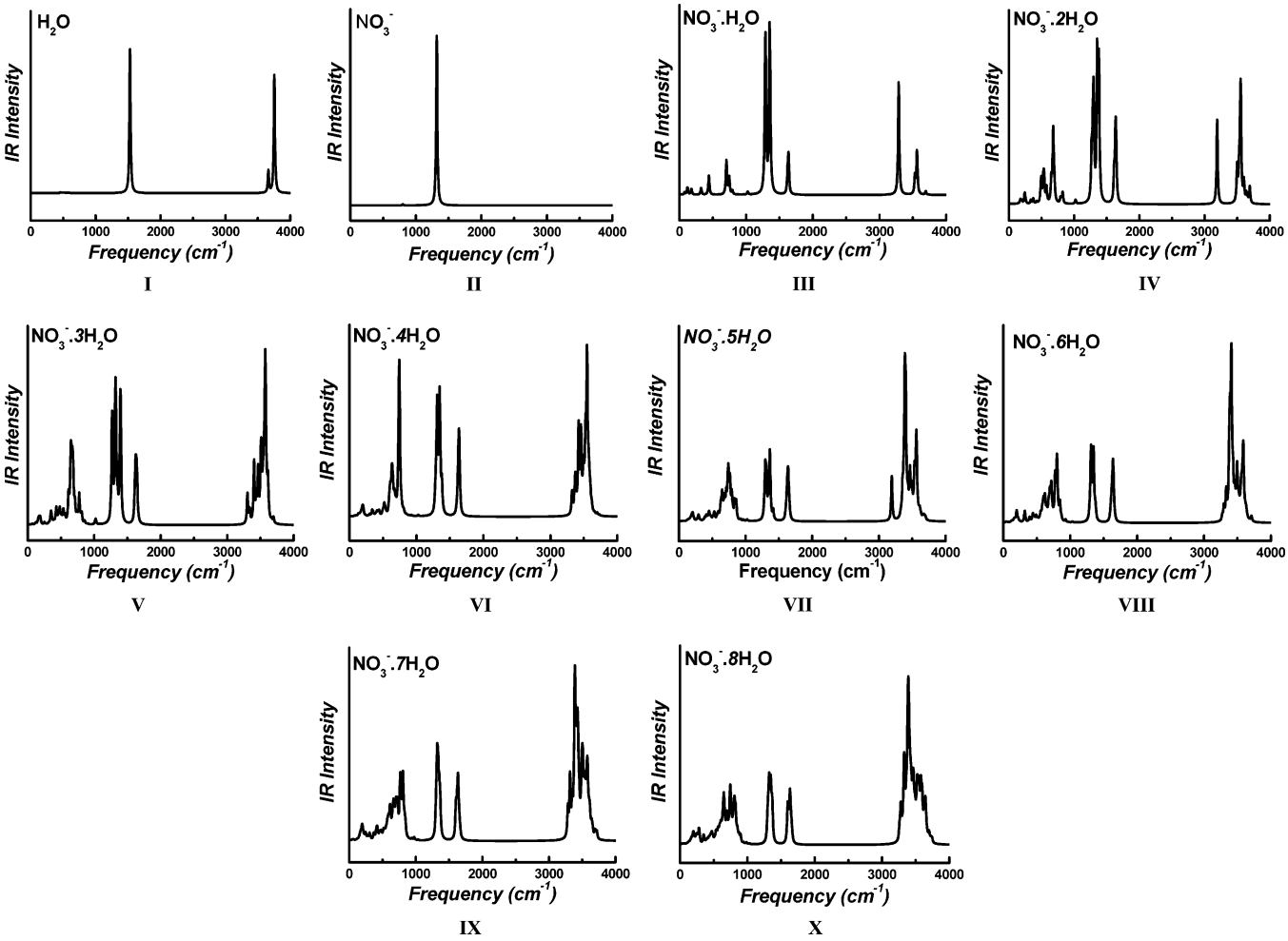

Figure 4. Calculated scaled IR spectra for (I) free H_2O and (II) free NO_3^- at B3LYP/6-311++G(d,p) level of theory. Scaled weighted average IR spectra for (III) $NO_3^-\cdot H_2O$, (IV) $NO_3^-\cdot 2H_2O$, (V) $NO_3^-\cdot 3H_2O$, (VI) $NO_3^-\cdot 4H_2O$, (VII) $NO_3^-\cdot 5H_2O$, (VIII) $NO_3^-\cdot 6H_2O$, (IX) $NO_3^-\cdot 7H_2O$, and (X) $NO_3^-\cdot 8H_2O$ hydrated clusters at the same level. The scaling factor is taken as 0.96 to account for the anharmonic nature of O−H stretching vibration in H_2O. The weight factor is calculated on the basis of statistical population of individual conformer for a particular size of hydrated cluster at 150 K. Lorentzian line shape has been considered with peak half-width of 10 cm^{-1} for all the IR plots.

Table 1. It is clearly observed that the relative stability of the minimum energy structures is in the same order as predicted by MP2 results.

The calculated interaction energy is further improved incorporating correction due to basis set superposition error (BSSE) following counterpoise method.[49] In cases when the basis sets applied are not complete, the binding energies without BSSE correction tend to be overestimated, whereas those with BSSE correction tend to be underestimated mainly due to underestimation of dispersion energy. The median values between the BSSE-corrected and BSSE-uncorrected binding energies are often somewhat closer to the measured values.[6] At present, 50% of the calculated BSSE is taken into account to correct the calculated interaction energies and the corrected values are listed in Table 2. The plot showing the variation of BSSE-corrected E_w^{int} vs n is displayed in Figure 3c. It is observed that the BSSE correction reduces the calculated interaction energy by <5%.

3.3. IR Spectra. $NO_3^-\cdot nH_2O$ clusters are stabilized by the interaction between O atoms of NO_3^- moiety and H atoms from solvent H_2O molecules as well as inter-water H-bonding interactions among solvent H_2O units. Due to these interactions, it is expected that IR bands due to stretching and bending modes of H_2O in the hydrated clusters, $NO_3^-\cdot nH_2O$ ($n = 1-8$) get shifted compared to that of free water molecules. IR spectra for all the minimum energy structures of $NO_3^-\cdot nH_2O$ clusters ($n \leq 8$) along with free H_2O and free NO_3^- systems are calculated. Based on experimental data on stretching frequency of H_2O ($\nu_{sym} = 3657$ cm^{-1}, $\nu_{asym} = 3756$ cm^{-1}) and the present calculated values ($\nu_{sym} = 3816$ cm^{-1}, $\nu_{asym} = 3912$ cm^{-1}) at the B3LYP/6-311++G(d,p) level, a scaling factor of 0.96 is considered to account the anharmonic nature of stretching vibrations. This factor is calculated on the basis of the average difference of calculated symmetric and asymmetric stretching vibrations from the experimental values of free water molecule. The same scaling factor has been used for predicting IR spectrum of all these hydrated clusters. Lorentzian line shape with peak half-width of 10 cm^{-1} has been considered for all IR plots. Calculated scaled vibration frequencies for free water are 1531, 3663 and 3756 cm^{-1}, respectively, for bending (ν_{bend}), symmetrical stretching (ν_{sym}) and asymmetrical stretching (ν_{asym}) at the B3LYP/6-311++G(d,p) level of theory and the theoretical IR spectrum is displayed in Figure 4-I. The scaled IR spectrum for free NO_3^- with a single sharp peak at ~1300 cm^{-1} in the N−O stretching region is shown in Figure 4-II. Calculated scaled O−H stretching frequencies for the most stable structure of each size (n) hydrated NO_3^- clusters are listed in Table 3.

Weight factors calculated for monohydrated cluster at 150 K suggest that two minimum energy configurations are present in the ratio of 60:40 at this temperature. The weighted average scaled IR spectrum for the monohydrate cluster, $NO_3^-\cdot H_2O$, is displayed in Figure 4-III. The spectrum shows two strong and sharp bands at 3290 and 3552 cm^{-1} in O−H stretching region

TABLE 3: Scaled O−H Stretching Frequency of H_2O Calculated at the B3LYP/6-311++G(d,p) Level of Theory for the Most Stable Conformer of $NO_3^-\cdot nH_2O$ Clusters ($n = 1-8$)[a]

$NO_3^-\cdot nH_2O$[b]	O−H stretching frequency (cm^{-1})
$NO_3^-\cdot H_2O$ structure IA	3552, 3563
$NO_3^-\cdot 2H_2O$ structure IIA	3552, 3557, 3640, 3692
$NO_3^-\cdot 3H_2O$ structure IIIA	3405, 3466, 3513, 3574, 3578, 3613
$NO_3^-\cdot 4H_2O$ structure IVA	3375, 3424, 3458, 3496, 3514, 3525, 3529, 3549
$NO_3^-\cdot 5H_2O$ structure VA	3325, 3355, 3389, 3400, 3427, 3468, 3530, 3538, 3565, 3672
$NO_3^-\cdot 6H_2O$ structure VIA	3333, 3378, 3390, 3409, 3433, 3460, 3494, 3550, 3560, 3571, 3587, 3710
$NO_3^-\cdot 7H_2O$ structure VIIA	3283, 3318, 3388, 3399, 3423, 3433, 3436, 3503, 3505, 3562, 3566, 3582, 3592, 3692
$NO_3^-\cdot 8H_2O$ structure VIIIA	3278, 3330, 3357, 3394, 3402, 3413, 3420, 3456, 3509, 3516, 3522, 3588, 3596, 3692, 3694, 3700

[a] The scaling factor applied to for account the anharmonic nature of stretching frequency is 0.96. [b] Structure of $NO_3^-\cdot nH_2O$ clusters are shown in Figure 2.

of water corresponding to asymmetric stretching vibrations of H_2O in structures I-B and I-A (see Figure 2), respectively, for the H-bonded O−H bonds. A very weak band observed at 3694 cm^{-1} corresponds to the asymmetric stretching vibration of H_2O in structure I-B for the spectator O−H bond. A large shift ($\Delta\nu \sim -450$ cm^{-1}) is observed for the O−H stretching band in case of single H-bonded (SHB) O−H bond of water (structure I-B) compared to a relatively small shift ($\Delta\nu \sim -60$ cm^{-1}) in the case of the spectator O−H bond. In the case of double H-bonded (DHB) O−H bonds (structure I-A), calculated IR shifts ($\Delta\nu$) for stretching modes observed are ~ -200 cm^{-1}. The IR band at 1640 cm^{-1} corresponding to the bending mode of water in both structures is shifted ($\Delta\nu$) by around $+100$ cm^{-1}. Two IR bands are observed for N═O stretching modes; the band related to free N═O bond is shifted by $+50$ cm^{-1} compared to the -15 cm^{-1} shift due to bonded N═O bond. The IR band at $\sim$800 cm^{-1} corresponds to the N inversion mode of NO_3^- in both structures. IR bands at $\sim$710 and 750 cm^{-1} correspond to wagging H atoms in structures I-A and I-B, respectively. IR bands below 500 cm^{-1} are due to librations of water.

The weighted average scaled IR spectrum of larger $NO_3^-\cdot nH_2O$ clusters ($n = 2-6$) are provided in Figure 4 (IV−X). It is observed that in all these hydrated clusters, the most stable structure (structure A) has a large relative population (50−70%) except for $NO_3^-\cdot 7H_2O$ and $NO_3^-\cdot 8H_2O$ systems at 150 K. In septa- and octahydrated clusters, no single minimum energy configuration has a relative population of >30% at this temperature. Thus, weighted average IR spectra of $NO_3^-\cdot 7H_2O$ and $NO_3^-\cdot 8H_2O$ systems have significant contributions from many minimum energy configurations. As a result, calculated IR spectra are more complex and the bands are not resolved except in the range of N═O stretching and water bending.

Apart from single and double hydrogen-bonded arrangements, an interwater H-bonding does exist in the dihydrated cluster (structure II-B). The IR band corresponding to the stretching mode of the O−H bond in which the H atom is at the H-bonding distance with the O atom of the second solvent unit is predicted at $\sim$3600 cm^{-1} in this structure. The largely shifted IR band in the O−H stretching region observed at $\sim$3190 cm^{-1} corresponds to a single H-bonded O−H stretching mode of the solvent water unit, which has a free H atom in the same structure. The single H-bonded O−H bond of the second solvent water molecule results a IR band at $\sim$3500 cm^{-1}. IR bands related to double H-bonded O−H bonds are observed in the range 3530−3690 cm^{-1}. The next IR band in the lower side of the spectrum as shown in Figure 4-IV at $\sim$1650 cm^{-1} is due to water bending in the dihydrate cluster. Two strong and sharp bands at $\sim$1300 cm^{-1} are due to asymmetric stretching vibrations of N═O bonds of the solute. A small band at $\sim$1000 cm^{-1} is due to symmetric stretching vibrations of N═O bonds in NO_3^- anion. IR bands below 800 cm^{-1} correspond to N inversion mode of NO_3^-, wagging H atoms and librations of water.

Weight factors calculated for trihydrated cluster at 150 K suggest that out of five predicted minimum energy structures, structures III-A and III-B having cyclic three-member inter-water H-bonding arrangements have major contributions. The weighted average scaled IR spectrum for cluster $NO_3^-\cdot 3H_2O$ is displayed in Figure 4-V. The spectrum shows overlapping bands in the range 3340−3700 cm^{-1} due to O−H stretching vibrations of water under different local environments. Normal-mode analysis suggests that these modes are coupled in all the minimum energy structures. In case of structure III-B, an IR band is observed at 3464 cm^{-1} corresponding to simultaneous symmetric stretching vibrations of O−H bonds in all the three solvent water molecules forming inter-water H-bonded cyclic network. The IR band due to the bending mode of water is observed at 1650 cm^{-1}. IR bands corresponding to asymmetric N═O stretching modes are obtained in the range 1270−1390 cm^{-1} of the spectrum. In the trihydrate cluster also, a small band at $\sim$1000 cm^{-1} is seen due to symmetric stretching vibrations of N═O bonds in the NO_3^- anion. IR bands below 800 cm^{-1} correspond to the N inversion mode of NO_3^-, wagging H atoms and librations of water as has been discussed.

In the case of the $NO_3^-\cdot 4H_2O$ cluster, the most stable structure (IV-A) has major contribution (>70%) at 150 K and the calculated IR spectrum is displayed in Figure 4-VI. Again, the spectrum shows overlapping bands in the range 3350−3650 cm^{-1} due to O−H stretching vibrations of water. Simultaneous symmetric stretching vibrations of O−H bonds in all four solvent water molecules forming inter-water H-bonded cyclic network correspond to an IR band at $\sim$3375 cm^{-1}. The IR band due to the bending mode of water is observed at $\sim$1650 cm^{-1}. IR bands corresponding to asymmetric N═O stretching modes are now overlapped to become almost a single sharp peak at $\sim$1325 cm^{-1}. The symmetric stretching vibration of N═O bonds in NO_3^- anion calculated at $\sim$1000 cm^{-1} is with very small intensity to be observed. Bands due to the N inversion mode of

NO_3^-, wagging H atoms and librations of water are observed below 800 cm^{-1}.

The weighted average IR spectrum calculated for the $NO_3^-\cdot 5H_2O$ cluster is displayed in Figure 4-VII. The spectrum shows overlapping bands in the range 3200−3700 cm^{-1} due to the O−H stretching vibrations of water. In the O−H stretching region of water, the largest shifted IR band at ∼3200 cm^{-1} corresponds to the O−H bond connected by inter-water H-bonding to make a five-member cyclic network (structure V-B). The bending mode of solvent water molecules in the cluster generates an IR band at ∼1650 cm^{-1}. IR bands corresponding to asymmetric N═O stretching modes are observed at ∼1305−1345 cm^{-1}. Bands due to wagging H atoms and librations of water are observed below 900 cm^{-1}. The N inversion mode of NO_3^- gives an IR band at ∼800 cm^{-1}. The essential feature in the calculated IR spectrum for $NO_3^-\cdot 6H_2O$ cluster as shown in Figure 4-VIII is similar to that of the pentahydrate cluster except there is no sharp resolved band at ∼3200 cm^{-1}. In the hexahydrate cluster, minimum energy configurations corresponding to interior structure are also predicted. It is observed that in the case of two interior structures (VI-D and VI-E), the N inversion mode of NO_3^- generates an IR band at ∼825 cm^{-1} in contrast to the same one at ∼800 cm^{-1} in the case of surface structures.

In the case of hepta- and octahydrated clusters, contributions from many minimum energy structures are significant. Calculated weighted average IR spectra for two clusters are displayed in Figure 4-IX and Figure 4-X, respectively. The two spectra show similar features having overlapping bands in O−H stretching region of water. IR bands due to bending mode of water are observed at ∼1650 cm^{-1}. IR bands corresponding to the asymmetric N═O stretching modes produce a single sharp peak at ∼1325 cm^{-1}. Symmetric stretching vibrations of N═O bonds in NO_3^- anion calculated at ∼1000 cm^{-1} in both cases have very weak intensities. Bands due to the N inversion mode of NO_3^- are observed at around 800−825 cm^{-1}. The IR band for wagging H atoms and librations of solvent water units are observed below 800 cm^{-1}. Vibrational frequency calculations are also carried out including anharmonic corrections applying vibrational self-consistent field (VSCF) theory for mono- and dihydrated clusters. The O−H stretching frequencies in structure I-A are calculated as 3440, 3459 cm^{-1} and 3679, 3711 cm^{-1}, respectively, with and without anharmonic corrections. It is worth mentioning that CPU time required for this anharmonic vibration calculation is 3 orders of magnitude higher than the harmonic calculation. In the case of structure II-A, the O−H anharmoic stretching frequencies are calculated as 3440, 3448, 3345 and 3480 cm^{-1} compared to the harmonic frequencies at 3845, 3791, 3705 and 3700 cm^{-1}. Again the CPU time required for this anharmonic calculation is more than 5 orders of magnitude higher than the harmonic calculation.

4. Conclusions

Microhydration of nitrate anion, NO_3^-, is studied following first principle based electronic structure calculations. Structure, energy and IR spectra of $NO_3^-\cdot nH_2O$ clusters ($n = 1-8$) are reported. Becke's three-parameter nonlocal exchange (B3) and Lee−Yang−Parr (LYP) nonlocal correlation functionals (B3LYP) as well as the MP2 method have been applied to study the present systems with split valence 6-311++G(d,p) basis functions. Several closely lying minimum energy structures are predicted. A structure having a H-bonded water network is observed to be more stable over the other structures where solvent H_2O units are connected to the NO_3^- moiety independently either by single or by double H-bonding. The excess electron is distributed equally over the three oxygen atoms of NO_3^-. The hydrated clusters of NO_3^- are bound by symmetrical dihydrogen bonding (DHB), single hydrogen bonding (SHB), and inter-water H bonding (WHB) interactions. It is also observed that up to five solvent H_2O units can reside around the solute in a cyclic inter-water hydrogen-bonding network. For higher clusters, a few minimum energy configurations are predicted having interior structures. Energy parameters, solvation and interaction energy are reported for $NO_3^-\cdot nH_2O$ clusters. Weighted average solvent stabilization energies are calculated on the basis of statistical population of different minimum energy structures at 150 K. Calculated vibration frequencies of the clusters illustrate that the formation of NO_3^-−water clusters induces shifts from the normal stretching modes of isolated water depending on local environments. Bending modes of solvent water units are not significantly affected. Weighted average IR spectra of each size of hydrated cluster are also calculated on the basis of the statistical population at 150 K.

Acknowledgment. We thank computer center, BARC for providing ANUPAM parallel computing facility. A.K.P. and D.K.M. thank Dr. S. K. Sarkar and Dr. S. K. Ghosh for their constant encouragement. We sincerely thank Dr. Savita Ladage, Homi Bhabha Centre for Science Education, for BSSE calculations applying Gaussian 03.

References and Notes

(1) Ohtaki, H.; Radani, T. *Chem. Rev.* **199**3, *93*, 1157.
(2) Marcus, Y. *Chem. Rev.* **1988**, *88*, 1475.
(3) Illenberger, E. *Chem. Rev.* **1992**, *92*, 1589.
(4) Simons, J.; Jordan, K. D. *Chem. Rev.* **1987**, *87*, 535.
(5) Majumdar, D.; Kim, J.; Kim, K. S. *J. Chem. Phys.* **2000**, *112*, 101.
(6) Kim, J.; Lee, H. M.; Suh, S. B.; Majumdar, D.; Kim, K. S. *J. Chem. Phys.* **2000**, *113*, 5259.
(7) Ayala, R.; Martinez, J. M.; Pappalardo, R. R.; Marcos, E. S. *J. Chem. Phys.* **2003**, *119*, 9538.
(8) Lee, H. M.; Kim, D.; Kim, K. S. *J. Chem. Phys*. **2002**, *116*, 5509.
(9) Ayala, R.; Martinez, J. M.; Pappalardo, R. R.; Marcos, E. S. *J. Phys. Chem. A* **2000**, *104*, 2799.
(10) Ayala, R.; Martinez, J. M.; Pappalardo, R. R.; Saint-Martin, H.; Ortega-Blake, I.; Marcos, E. S. *J. Chem. Phys*. **2002**, *117*, 10512.
(11) Bryce, R. A.; Vincent, M. A.; Malcolm, N. O. J.; Hillier, I. H. *J. Chem. Phys.* **1998**, *109*, 3077.
(12) Vaughn, S. J.; Akhmatskaya, E. V.; Vincent, M. A.; Masters, A. J.; Hillier, I. H. *J. Chem. Phys.* **1999**, *110*, 4338.
(13) Ignaczak, A.; Gomes, J. A. N. F.; Cordeiro, M. N. D. S. *Electrochim. Acta* **1999**, *45*, 659.
(14) Lehr, L.; Zannai, M. T.; Frischkorn, C.; Weinkauf, R.; Neumark, D. M. *Science* **1999**, *284*, 635.
(15) Dang, L. X.; Garret, B. C. *J. Chem. Phys.* **1993**, *99*, 2972.
(16) Gai, H.; Schenter, G. K.; Dang, L. X.; Garret, B. C. *J. Chem. Phys.* **1996**, *105*, 8835.
(17) Markovich, G.; Pollac, S.; Giniger, R.; Cheshnovosky, O. *J. Chem. Phys.* **1994**, *101*, 9344.
(18) Markovich, G.; Pollac, S.; Giniger, R.; Cheshnovosky, *Z. Phys. D: At. Mol. Clustres* **1993**, *26*, 98.
(19) Ayala, R.; Martinez, J. M.; Pappalardo, R. R.; Marcos, E. S. *J. Chem. Phys.* **2004**, *121*, 7269.
(20) Ayotte, P.; Weddle, G. H.; Kim, J.; Johnson, M. A. *J. Am. Chem. Soc.* **1998**, *120*, 12361.
(21) Robertson, W. H.; Diken, E. G.; Price, E. A.; Shin, J. W.; Johnson, M. A. *Science* **2003**, *299*, 1367.
(22) Xantheas, S. S. *J. Am. Chem. Soc.* **1995**, *117*, 10373.
(23) Weber, J. M.; Kelley, J. A.; Nielson, S. B.; Ayotte, P.; Johnson, M. A. *Science* **2000**, *287*, 2461.
(24) Weber, J. M.; Kelley, J. A.; Robertson, W. H.; Johnson, M. A. *J. Chem. Phys.* **2001**, *114*, 2698.
(25) Myshakin, E. M.; Jordan, K. D.; Robertson, W. H.; Weddlle, G. H.; Johnson, M. A. *J. Chem. Phys.* **2003**, *118*, 4945.
(26) Pathak, A. K.; Mukherjee, T.; Maity, D. K. *J. Chem. Phys.* **2006**, *125*, 074309.
(27) Price, E. A.; Hammeer, N. I.; Johnson, M. A. *J. Phys. Chem. A* **2004**, *108*, 3910.

(28) Pathak, A. K.; Mukherjee, T.; Maity, D. K. *J. Chem. Phys.* **2006**, *124*, 024322.
(29) Pathak, A. K.; Mukherjee, T.; Maity, D. K. *J. Chem. Phys.* **2007**, *127*, 044304.
(30) Pathak, A. K.; Mukherjee, T.; Maity, D. K. *J. Chem. Phys.* **200**7, *126*, 034301.
(31) Zhou, J.; Santambrogio, G.; Brummer, M.; Moore, D. T.; Woste, L.; Meijer, G.; Neumark, D. M.; Asmis, K. R. *J. Chem. Phys.* **2006**, *125*, 111102.
(32) Wang, X. B.; Nicholas, J. B.; Wang, L. S. *J. Chem. Phys.* **2000**, *113*, 10837.
(33) Kelley, C. P.; Cramer, C. J.; Truhlar, D. G. *J. Phys. Chem. A* **2006**, *110*, 2493.
(34) Wayne, R. P. *Chemistry of Atmospheres*; Oxford University Press: Oxford, U.K., 2000.
(35) Finlayson-Pitts, B. J.; Pitts, J. N. *Chemistry of the Upper and Lower Atmosphere*; Academic: San Diego, 2000.
(36) Bickmore, B. R.; Nagy, K. L.; Young, J. S.; Drexler, J. W. *Environ. Sci. Technol.* **2001**, *35*, 4481.
(37) Chambliss, C. K.; Haverlock, T. J.; Bonnesen, P. V.; Engle, N. L.; Moyer, B. A. *Environ. Sci. Technol.* **2002**, *36*, 1861.
(38) Wang, X. B.; Yang, X.; Wang, L. S.; Nicholas, J. B. *J. Chem. Phys.* **2002**, *116*, 561.
(39) Waterland, M. R.; Stockwell, D.; Kelley, A. M. *J. Chem. Phys.* **2001**, *114*, 6249.
(40) Howell, J. M.; Sapse, A. M.; Singman, E.; Snydar, G. *J. Phys. Chem.* **1982**, *86*, 2345.
(41) Shen, M.; Xie, Y.; Schaefer, H. F., III; Deakyne, C. A. *J. Chem. Phys.* **1990**, *93*, 3379.
(42) Dang, L. X.; Chang, T. M.; Roeselova, M.; Garrett, B. C.; Tobias, D. J. *J. Chem. Phys.* **2006**, *124*, 066101.
(43) Tongraar, A.; Tangkawanwanit, P.; Rode, B. M. *J. Phys. Chem. A* **2006**, *110*, 12918.
(44) Ebner, C.; Sansone, R.; Probst, M. *Int. J. Quant. Chem.* **1998**, *70*, 877.
(45) Becke, A. D. *J. Chem. Phys.* **1993**, *90*, 5648.
(46) Schmidt, M. W.; Baldridge, K. K.; Boatz, J. A.; Elbert, S. T.; Gordon, M. S.; Jensen, J. H.; Koseki, S.; Matsunaga, N.; Nguyen, K. A.; Su, S. J.; Windus, T. L.; Dupuis, M.; Montgomery, J. A. *J. Comput. Chem.* **1993**, *14*, 1347.
(47) Schaftenaar, G.; Noordik, J. H. *J. Comp.-Aided Mol. Des.* **2000**, *14*, 123.
(48) Lee, N.; Keesee, R. G.; Castleman, A. W., Jr. *J. Chem. Phys.* **1980**, *72*, 1089.
(49) Boys, S. F.; Bernardi, F. *Mol. Phys.* **1970**, *19*, 553.